the values of ΔU_{obsd}(Cu–N2) are significantly negative (Table IV). Qualitatively these observations may be explained as follows: The site symmetry of the cation is C_1, i.e., there is no reason that the positions of the Cu atoms in the disordered molecules I and II are the same (Figure 1). If we assume that the transition I $\rightleftarrows$ II is accompanied by a shift δ of Cu approximately in the direction of O2, the following relationship may be obtained

$$\Delta U_{dis}(\text{Cu–O2}) = [\Delta d^2(\text{Cu–O2}) - (\Delta d(\text{Cu–O2}))^2]\,[1 + \delta/\Delta d(\text{Cu–O2})]$$

$$\Delta U_{dis}(\text{Cu–N2}) = [\Delta d^2(\text{Cu–N2}) - (\Delta d(\text{Cu–N2}))^2]\,[1 - v/\Delta d(\text{Cu–N2})]$$

By using observed values for Δd, (Δd), and $\Delta U_{obsd} - 0.003$ Å^2 $\approx \Delta U_{dis}$, δ is calculated to be $\sim$0.4 Å from ΔU_{obsd}(Cu–O2) and $\sim$0.2 Å from ΔU_{obsd}(Cu–N2). The two estimates do not agree very well but at least they have the same sign and order of magnitude.

A similar analysis for the dependence of $\Delta U_{obsd}(\text{Cu–N}_{eq})$ on $(\Delta d(\text{Cu–N}))$ for N1 and N2 does not give significant results because the value of ΔU_{dis}(Cu–N) estimated from Δd(Cu–N) is $\sim$0.005 Å^2, approximately the same as the root-mean-square standard deviation of U_{obsd}(Cu–N) ($\sim$0.004 Å^2).

Conclusion

The data sets [CuO3] to [CuO6] all pertain to $[Cu^{II}(bipy)_2ONO]NO_3$ measured by diffractometry at 298, 165, 100, and 20 K. (⊛ in Figure 4). The site symmetry of Cu is C_1, the energy difference E between I and II (Figure 1) is $\sim$150 cm^{-1}, and the population factor P therefore depends on T.[14] As Figure 4 shows the corresponding data points nicely follow the regression curve. This indicates that the energy barrier between I and II is sufficiently small to allow equilibration and that the disorder, at least for this compound, is dynamic rather than static. For the data sets [Cu24] and [Cu25] pertaining to $[Cu^{II}phen_2CH_3COO]ClO_4$ measured at 298 and 165 K the case for dynamic disorder is less convincing.

In summary, the variation in d(Cu–O) and ΔU_{obsd}(Cu–O) may be largely explained in terms of a simple geometrical model for the automerization between the two forms of the $[Cu^{II}(LL)_2X]^+$ ion (I, II, Figure 1). This provides additional support to the potential energy curve and the underlying geometrical model of the pseudo-Jahn–Teller distortion. Deviations from this model are either due to its simplistic nature or to the limited accuracy of U_{obsd}.

The present analysis is another example in a series of interpretations of ΔU_{obsd} values[5] from routine structure determinations. Other studies were concerned with Jahn–Teller distortions of $Cu^{II}N_6$ and $Mn^{III}F_6$ coordination octahedra,[5b,16] with spin changes in $Fe^{III}S_6$ coordination octahedra[5c] and with valence disorder in a binuclear N_4Mn^{III}–(μ-O)$_2$–$Mn^{IV}N_4$ complex.[17] These studies show that for crystal structure analysis of coordination compounds done with average accuracy values of ΔU_{obsd} in the range 0.2–0.003 Å^2 are amenable to chemical interpretation. For compounds containing first-row atoms only, ΔU_{obsd} as low as 0.001 Å^2 may still be chemically meaningful, if accurate diffraction data to high scattering angle are interpreted in terms of multipole models of the molecular electron density function.[18]

Acknowledgment. We appreciate the cooperation of Prof. C. J. Simmons and Prof. B. J. Hathaway in promptly providing unpublished data. We acknowledge the comments of a referee.

Supplementary Material Available: A table summarizing details of data collection and refinement (1 page). Ordering information is given on any current masthead page.

(16) Vedani, A. Ph.D. Thesis, University of Zürich, 1981.
(17) (a) Stebler, M.; Ludi, A.; Bürgi, H. B. *Inorg. Chem.* **1986**, *22*, 4743. (b) Stebler, M. Ph.D. Thesis, University of Bern, 1986.
(18) Bürgi, H. B., in preparation.

Alkyne Ligands as Two-Electron Donors in Octahedral d^6 Tungsten(0) Complexes: *fac*-W(CO)$_3$(dppe)(η^2-HC≡CR) and W(CO)$_2$(dppe)(DMAC)$_2$

K. R. Birdwhistell, T. L. Tonker, and J. L. Templeton*

Contribution from the W. R. Kenan, Jr. Laboratory, Department of Chemistry, University of North Carolina, Chapel Hill, North Carolina 27514. *Received July 3, 1986*

Abstract: Three labile terminal alkyne adducts of tungsten(0), *fac*-W(CO)$_3$(dppe)(η^2-HC≡CR) (dppe = $Ph_2PCH_2CH_2PPh_2$; R = H, *n*-Bu, and Ph) have been synthesized from *fac*-W(CO)$_3$(dppe)(acetone). Chemical and spectroscopic properties indicate that the alkyne ligand is weakly bound in these octahedral d^6 monomers. Recognition of an unfavorable 2-center-4-electron repulsion between the filled alkyne $\pi_\perp$ orbital and a filled metal dπ orbital helps to rationalize the observed chemistry. Internal alkyl and aryl alkynes do not yield clean products under similar reaction conditions, but the electron poor ester substituted alkyne DMAC (DMAC = dimethylacetylenedicarboxylate) forms W(CO)$_2$(dppe)(DMAC)$_2$. A single-crystal X-ray study of this complex confirmed the trans alkyne–cis dicarbonyl geometry anticipated from spectroscopic data [space group $P\bar{1}$, a = 11.51 (1) Å, b = 18.90 (1) Å, c = 10.27 (1) Å, α = 102.74 (6)°, β = 107.90 (8)°, γ = 79.95 (8)°, Z = 2, R = 0.035, R_w = 0.047 for 6000 unique data with $I > 3\sigma(I)$]. The two trans alkyne ligands are orthogonal to one another with each alkyne eclipsing one of the two P–W–C vectors of the equatorial W(CO)$_2$(dppe) unit. Dynamic ^{1}H NMR studies reveal a barrier of 17.7 kcal/mol for averaging the two ends of each DMAC ligand, presumably by an alkyne rotation process. The role of alkyne ester substituents in promoting dπ to $\pi_\parallel$* backbonding *and* delocalizing $\pi_\perp$ alkyne electrons away from dπ metal electron density is discussed. These results help to rationalize three general features of transition-metal alkyne chemistry: (i) two-electron donor DMAC analogues of metal–olefin complexes are common; (ii) d^6 metal octahedra promote isomerization of terminal alkyne ligands to vinylidenes, and (iii) terminal and dialkyl alkyne ligands prefer to bind to high oxidation state metals having at least one vacant dπ orbital.

Numerous octahedral molybdenum and tungsten d^4 monomers contain one[1] or two[2] tightly bound alkyne ligands. The d^2 configuration is also well represented among octahedral molybdenum[3] and tungsten[4] complexes containing an alkyne ligand. Both of

0002-7863/87/1509-1401$01.50/0 © 1987 American Chemical Society

these configurations allow the filled alkyne $\pi_\perp$ orbital to encounter a vacant $d\pi$ orbital. Donation from the alkyne $\pi_\perp$ orbital influences molecular structure and reactivity[5] as well as spectroscopic properties in these complexes.[6]

Although six-coordinate d^6 complexes serve as a paradigm for application of 18-electron guidelines, there are surprisingly few Group 6 d^6 octahedra containing an alkyne ligand. Early work with molybdenum(0) and tungsten(0) alkyne derivatives was characterized by unusual stoichiometries. The synthesis,[7] structure,[8] and molecular orbital scheme[9] reported for $W(CO)(RC_2R)_3$ laid the foundation for much of the Group 6 work which has followed. Work with chromium has produced unusual stoichiometries[10] as well as alkyne adducts corresponding to effective atomic number expectations: $Cr(CO)_5(\eta^2\text{-HC}{\equiv}CCO_2Me)$[11] and $(\eta^6\text{-}C_6Me_6)Cr(CO)_2(\eta^2\text{-PhC}{\equiv}CPh)$.[12] The alkyne ligands in these last two d^6 saturated complexes are labile, as are alkynes in related six-coordinate complexes of Mn(I)[13] and Fe(II).[14] Although the d^6 $(\pi\text{-}C_5H_5)Re(CO)_2(PhC_2Ph)$ complex recently reported resists alkyne substitution, the bound alkyne is one of the least geometrically perturbed from free PhC≡CPh of any structurally characterized diphenylacetylene complex.[15]

Our understanding of the physical and chemical properties of six-coordinate d^6 complexes containing alkyne ligands is still minimal. How is the alkyne $\pi_\perp$ electron pair accommodated when all three of the octahedral $d\pi$ orbitals are filled? Do the alkyne $\pi_\perp$ electrons influence the orientational preference or the reactivity patterns of d^6 $L_5M(\eta^2\text{-RC}{\equiv}CR)$ complexes? Are five-coordinate geometries accessible for d^6 configurations in order to provide a vacant metal orbital mate for the filled $\pi_\perp$ alkyne orbital? The preparation and properties of *fac*-$W(CO)_3(dppe)(\eta^2\text{-HC}{\equiv}CR)$ [R = H (**2a**), Ph (**2b**), and *n*-Bu (**2c**)] and $W(CO)_2(dppe)(DMAC)_2$ (**3**) [DMAC = $MeO_2CC{\equiv}CCO_2Me$] address these questions.

Experimental Section

Materials and Methods. All manipulations were performed under a dry nitrogen atmosphere by using standard Schlenk techniques. Methylene chloride was distilled from $LiAlH_4$; diethyl ether and tetrahydrofuran were distilled from sodium benzophenone ketyl and purged with nitrogen. All other solvents were purged with nitrogen and used without further purification. Tungsten and molybdenum hexacarbonyl and alkyne reagents were used as obtained from commercial sources. $W(CO)_4(dppe)$[16] and *fac*-$W(CO)_3(dppe)(acetone)$[17] were prepared by literature methods.

Infrared spectra were recorded on a Beckman IR 4250 spectrometer and calibrated with a polystyrene standard. ^1H NMR spectra were recorded on a Varian XL-100 (100-MHz) or a Bruker WM 250 (250-MHz) spectrometer. ^{13}C NMR (62.89-MHz) and ^{31}P NMR (101.27-MHz) were also obtained on a Bruker WM 250 spectrometer. Variable temperature ^1H NMR were recorded on a Varian XL-100 by using a methanol thermometer located in the probe for temperature determination. All ^{31}P spectra were ^1H decoupled. Chemical shifts were referenced to residual solvent protons for ^1H NMR, to the chemical shift of the solvent for ^{13}C NMR, and to external phosphoric acid for ^{31}P NMR. Electrochemical measurements were obtained on a Bioanalytical Systems Inc. Model CV-27 instrument by using dichloromethane solutions containing 0.2 M tetra-*n*-butylammonium perchlorate (TBAP) as supporting electrolyte. $E(1/2)$ values $[(E_{p,a} + E_{p,c})/2]$ were recorded against a silver/silver chloride reference electrode. Ferrocene was used as an internal standard for potential calibration. All photolyses were carried out in a submersion type photolysis apparatus at 0 °C by using a Hanovia 750-W medium-pressure Hg arc lamp with a Pyrex filter and a continuous nitrogen purge.

***fac*-W(CO)$_3$(dppe)(HCCH) (2a).** A 500-mL flask was charged with *fac*-$W(CO)_3(dppe)(acetone)$ (2.76 mmol, 2.00 g) and 1 atm of acetylene (acetone stabilizer was removed by passing the acetylene gas through a −78 °C trap). Addition of 20 mL of toluene resulted in conversion to a dark yellow solution of *fac*-$W(CO)_3(dppe)(HCCH)$. The product was isolated as a yellow powder in 90% yield by filtering the toluene solution into 100 mL of hexanes and washing the yellowish orange powder which precipitated with pentanes (3 × 30 mL): IR (thf) ν(CO) (cm^{-1}) 1961 s, 1888 s, 1852 s; IR (KBr) 1942 s, 1862 s, 1822 s; ^1H NMR (CD_2Cl_2) 8.06–7.82 (m, Ph), 5.78 (t, $^3J_{HP}$ = 4 Hz, HC_2H), 2.60 (m, PCH_2CH_2P). Anal. Found (Calcd): C, 53.78 (53.79); H, 3.97 (3.78); W, 25.98 (26.56).

***fac*-W(CO)$_3$(dppe)(PhCCH) (2b).** To *fac*-$W(CO)_3(dppe)(acetone)$ (1.01 mmol, 0.73 g) was added a solution of PhC_2H (3.40 mmol, 0.35 g) in 10 mL of toluene. This mixture was stirred at room temperature until the reaction was complete as monitored by IR. The reaction solution was then cooled to 0 °C and filtered into 80 mL of dry hexanes to produce a pink, powdery solid. The solid was isolated, washed 3 × 30 mL of hexanes, and dried in vacuo (84% yield): IR (thf) ν(CO) (cm^{-1}) 1967 s, 1894 s, 1855 s; IR (KBr) 1961 s, 1890 s, 1835 s; ^1H NMR (benzene-d_6) δ 8.29–7.03 (m, Ph), 6.21 (t, $^3J_{HP}$ = 12 Hz, $^2J_{HW}$ = 6 Hz, PhC_2H), 2.68 (m, PCH_2CH_2P); ^1H NMR (CD_2Cl_2) δ 7.90–6.88 (m, Ph), 6.76 (t, $^3J_{HP}$ = 12 Hz, PhC_2H), 2.68 (m, PCH_2CH_2P); $^{31}P\{^1H\}$ NMR (THF/10% benzene-d_6) δ 37.6 (s, $^1J_{PW}$ = 204 Hz); ^{13}C NMR at 2 °C in the presence of PhC_2H (benzene-d_6) δ 221.8 (t, $^2J_{CP}$ = 8 Hz, CO trans to alkyne), 213.3 (dd, $^2J_{CP}$ = 26, 9 Hz, 2 cis CO), 135.6–121.4 (Ph), 98.2 (d, $^2J_{CH}$ = 27 Hz, PhCCH), 88.7 (dt, $^1J_{CH}$ = 231 Hz, $^2J_{CP}$ = 10 Hz, PhCCH), 27.3 (tt, $^1J_{CH}$ = 126 Hz, $^1J_{CP}$ = 19 Hz, PCH_2CH_2P). Anal. Found (Calcd): C, 58.57 (57.84); H, 4.17 (3.94); W, 23.57 (23.93).

***fac*-W(CO)$_3$(dppe)(HCC(CH$_2$)$_3$CH$_3$) (2c).** The preparation of **2c** was analogous to that of **2a**. **2c** was isolated as a yellow powder in 70% yield: IR (toluene) ν(CO) (cm^{-1}) 1960 s, 1885 s, 1850 s; IR (KBr) 1945 s, 1860 s, 1818 s; ^1H NMR (CD_2Cl_2) δ 8.00–6.70 (m, Ph), 4.49 (tt, $^3J_{HP}$ = 11 Hz, $^4J_{HH}$ = 2 Hz, RC_2H), 2.66 (m, PCH_2CH_2P), 1.23 (m, $-CH_2CH_2CH_2-$), 0.82 (m, CH_3); ^1H NMR (benzene-d_6) δ 7.83–6.67 (m, Ph), 4.61 (tt, $^3J_{HP}$ = 10 Hz, $^4J_{HH}$ = 2 Hz, RC_2H), 2.69 (br t, $^3J_{HH}$ = 6 Hz, C≡C—CH_2—CH_2Et), 2.14 (m, PCH_2CH_2P), 1.21 (br, m, C≡C—CH_2CH_2—Et), 0.77 (br, m, CH_2CH_3). Anal. Found (Calcd): C, 55.90 (56.17); H, 4.66 (4.58); W, 23.79 (24.57).

Reaction of 1-Hexyne with *fac*-W(CO)$_3$(dppe)(THF). Addition of a solution of *fac*-$W(CO)_3(dppe)(THF)$ (0.9 mmol) in 20 mL of THF to 1-hexyne (3.20 mmol) resulted in formation of a 1:1 mixture of *fac*-W-

(1) (a) Ricard, L.; Weiss, R.; Newton, W. E.; Chen, G. J.-J.; McDonald, J. W. *J. Am. Chem. Soc.* **1978**, *100*, 1318. (b) Allen, S. R.; Baker, P. K.; Barnes, S. G.; Green, M.; Trollope, L.; Manojlovic-Muir, L.; Muir, K. W. *J. Chem. Soc., Dalton Trans.* **1981**, 873. (c) Davidson, J. L.; Vasapollo, G. *J. Chem. Soc., Dalton Trans.* **1985**, 2239. (d) Alt, H. G. *J. Organomet. Chem.* **1977**, *127*, 349. (e) Umland, P.; Vahrenkamp, H. *Chem. Ber.* **1982**, *115*, 3580. (f) Winston, P. B.; Burgmayer, S. J. N.; Tonker, T. L.; Templeton, J. L. *Organometallics* **1986**, *5*, 1707. (g) Churchill, M. R.; Wasserman, H. J.; Holmes, S. J.; Schrock, R. R. *Organometallics* **1982**, *1*, 766. (h) Giandomenico, C. M.; Lam, C. T.; Lippard, S. J. *J. Am. Chem. Soc.* **1982**, *104*, 1263.

(2) (a) McDonald, J. W.; Newton, W. E.; Creedy, C. T. C.; Corbin, J. L. *J. Organomet. Chem.* **1975**, *92*, C25. (b) Herrick, R. S.; Templeton, J. L. *Organometallics* **1982**, *1*, 842. (c) Davidson, J. L.; Green, M.; Stone, F. G. A.; Welch, A. J. *J. Chem. Soc., Dalton Trans.* **1976**, 738. (d) Watson, P. L.; Bergman, R. G. *J. Am. Chem. Soc.* **1980**, *102*, 2698. (e) Faller, J. W.; Murray, H. H. *J. Organomet. Chem.* **1979**, *172*, 171. (f) Mead, K. A.; Morgan, H.; Woodward, P. *J. Chem. Soc., Dalton Trans.* **1983**, 271.

(3) (a) Maatta, E. A.; Wentworth, R. A. D.; Newton, W. E.; McDonald, J. W.; Watt, G. D. *J. Am. Chem. Soc.* **1978**, *100*, 1320. (b) Newton, W. E.; McDonald, J. W.; Corbin, J. L.; Ricard, L.; Weiss, R. *Inorg. Chem.* **1980**, *19*, 1997. (c) Braterman, P. S.; Davidson, J. L.; Sharp, D. W. A. *J. Chem. Soc., Dalton Trans.* **1976**, 241. (d) Howard, J. A. K.; Stansfield, R. F. D.; Woodward, P. *J. Chem. Soc., Dalton Trans.* **1976**, 246.

(4) (a) Bennett, M. A.; Boyd, I. W. *J. Organomet. Chem.* **1985**, *290*, 165. (b) Templeton, J. L.; Ward, B. C.; Chen, G. J.-J.; McDonald, J. W.; Newton, W. E. *Inorg. Chem.* **1981**, *20*, 1248. (c) Morrow, J. R.; Tonker, T. L.; Templeton, J. L. *Organometallics* **1985**, *4*, 745. (d) Bokiy, N. G.; Gatilov, Yu. V.; Struchkov, Yu. T.; Ustynyuk, N. A. *J. Organomet. Chem.* **1973**, *54*, 213.

(5) Herrick, R. S.; Leazer, D. M.; Templeton, J. L. *Organometallics* **1983**, *2*, 834.

(6) Templeton, J. L.; Herrick, R. S.; Morrow, J. R. *Organometallics* **1984**, *3*, 535.

(7) Tate, D. P.; Augl, J. M. *J. Am. Chem. Soc.* **1963**, *85*, 2174.

(8) Laine, R. M.; Moriarity, R. E.; Bau, R. *J. Am. Chem. Soc.* **1972**, *94*, 1402.

(9) (a) Tate, D. P.; Augl, J. M.; Ritchey, W. M.; Ross, B. L.; Grasselli, J. G. *J. Am. Chem. Soc.* **1964**, *86*, 3261. (b) King, R. B. *Inorg. Chem.* **1968**, *7*, 1044.

(10) Dotz, K. .; Mühlemeier, J. *Angew. Chem., Int. Ed. Engl.* **1982**, *21*, 929. (b) Wink, D. J.; Fox, J. R.; Cooper, N. J. *J. Am. Chem. Soc.* **1985**, *107*, 5012.

(11) Berke, H.; Harter, P.; Huttner, G.; Zsolnai, L. *Z. Naturforsch., B: Anorg. Chem., Org. Chem.* **1981**, *36B*, 929.

(12) Strohmeier, W.; Hellmann, H. *Chem. Ber.* **1965**, *98*, 1598.

(13) Antonova, A. B.; Kolobova, N. E.; Petrovsky, P. V.; Lokshin, B. V.; Obezyuk, N. S. *J. Organomet. Chem.* **1977**, *137*, 55.

(14) (a) Reger, D. L.; Coleman, C. J.; McElligott, P. J. *J. Organomet. Chem.* **1979**, *171*, 73. (b) Reger, D. L.; Belmore, K. A.; Mintz, E.; McElligott, P. J. *Organometallics* **1984**, *3*, 134.

(15) Einstein, F. W. B.; Tyers, K. G.; Sutton, D. *Organometallics* **1985**, *4*, 489.

(16) Grim, S. O.; Briggs, W. L.; Barth, R. C.; Tolman, C. A.; Jesson, J. P. *Inorg. Chem.* **1974**, *13*, 1095.

(17) Schenk, W. A.; Müller, H. *Chem. Ber.* **1982**, *115*, 3618.

Table I. Crystallographic Data for $W(CO)_2(dppe)(DMAC)_2$ (3)

formula	$WP_2O_{10}C_{40}H_{36}\cdot{}^1/_2CH_2Cl_2$
mol wt	964.94
space group	$P\bar{1}$
cell parameters	
a, Å	11.51 (1)
b, Å	18.90 (1)
c, Å	10.27 (1)
α, deg	102.74 (6)
β, deg	107.90 (8)
γ, deg	77.95 (8)
V, Å^3	2059.5
ρ (calcd), g/cm^3	1.62
Z	2
cryst color	yellow
radiatn (wavelength, Å)	Mo Kα (0.71073)
μ, absorptn coeff	32.4 cm^{-1}
scan type	$\omega/1.67\theta$
scan width	1.1 + 0.35 tan θ
background	25% of full scan width on both sides
θ limits	$3° < \theta < 28°$
hemisphere collctd	$+h\pm k\pm l$
no. of data	10359
no. of unique data used ($I > 3\sigma(I)$)	6000
no. of parameters	370
error in an observtn of unit wt	2.59
R	0.035
R_w	0.047

$(CO)_3(dppe)$(1-hexyne) and *fac*-$W(CO)_3(dppe)(THF)$ as judged by IR. The ratio of products remained unchanged for several hours at room temperature. Heating this mixture to 60 °C for 3 h precipitated a pale yellow solid. An IR of the solution showed $W(CO)_4(dppe)$ as the only carbonyl containing material left in solution. The pale yellow powder was identified as $\{[W(CO)_3(dppe)]_2(\mu\text{-dppe})\}$:[18] IR ($CH_2Cl_2$) ν(CO) (cm^{-1}) 1935 s, 1832 s; ^{31}P NMR (CH_2Cl_2) δ 34.4 (d, $^2J_{PP}$ = 22 Hz, 2 P), 8.5 (m, 1 P).

$W(CO)_2$(dppe)$(DMAC)_2$ (3) (DMAC = Dimethylacetylenedicarboxylate). To a mixture of solid *fac*-$W(CO)_3(dppe)$(acetone) (1.06 mmol, 0.77 g) and DMAC (3.9 mmol, 0.56 g) was added 30 mL of THF; a deep red solution resulted. The mixture was stirred at room temperature overnight, then solvent was removed, and the resulting oil was chromatographed on Florisil. The product eluted as the first yellow band after developing the column with CH_2Cl_2, a 1:1 ether:THF mixture, and THF. After solvent removal the light yellow oil can be recrystallized from CH_2Cl_2/hexane to give amber crystals in 26% yield. IR (thf) ν(CO) (cm^{-1}) 2030 s, 1980 s, ν(COO) 1730 m, 1700 m; IR (KBr) ν(CO) 2030 s, 1980 s, ν(COO) 1715 m, 1685 m; ^{1}H NMR (acetone-d_6) δ 8.00–6.92 (m, Ph), 3.58 (s, OMe, 6 H), 2.80 (m, PCH_2CH_2P), 2.74 (s, OMe, 6 H); ^{31}P{^{1}H} NMR (acetone-d_6) δ 27.5 (s, $^1J_{PW}$ = 187 Hz); ^{13}C{^{1}H} NMR (CD_2Cl_2) δ 202.0 (d, $^2J_{CP}$ = 61 Hz, 2 CO), 170.6 (s, *C*(O)(OMe), 166.5 (s, *C*(O)OMe), 138.0–126.9 (Ph and possibly bound alkyne carbons), 52.3 (s, C(O)O*C*H$_3$), 51.2 (s, C(O)O*C*H$_3$), 25.1 (m, $^2J_{CP}$ coupling, PCH_2CH_2P). Anal. Found (Calcd for $W(CO)_2(dppe)(DMAC)_2\cdot{}^1/_2CH_2Cl_2$): C, 49.20 (50.41); H, 4.12 (3.87); W, 18.82 (19.05).

Collection of Diffraction Data. A yellow prism having approximate dimensions 1.0 × 0.6 × 0.5 mm was mounted on a glass wand and coated with epoxy cement. Diffraction data were collected on an Enraf-Nonius CAD-4 automated diffractometer.[19] A triclinic cell was indicated from 25 centered reflections found in the region $30° < 2\theta < 35°$ and refined by least-squares calculations. The unit cell parameters are listed in Table I.

Diffraction data were collected in the hemisphere $+h\pm k\pm l$ under the conditions specified in Table I. Three reflections chosen as intensity standards were monitored every 3 h and showed no decay. The crystal was checked for orientation after every 300 reflections; recentering was never required. Four scans with nine reflections having $80° < \chi < 90°$ were performed to provide an empirical correction for absorption. The data were corrected for Lorentz-polarization effects, and 6000 reflections having $I > 3\sigma(I)$[20] were used in the structure solution and refinement.

Solution and Refinement of the Structure. The solution of the structure was straightforward from the application of the heavy atom method. The space group $P\bar{1}$ was deduced from the presence of two molecules per unit cell which were related by an inversion center. The tungsten atom was located in a three-dimensional Patterson function. The positions of the remaining non-hydrogen atoms were obtained from subsequent Fourier and difference Fourier calculations. One molecule of methylene chloride of solvation was also located in the unique portion of the unit cell.

Least-squares refinement[21] of the 56 non-hydrogen atoms allowing all except the methylene chloride and the phenyl carbons to vary anisotropically produced unweighted and weighted residuals of 6.3% and 7.1%, respectively.[22] The positions of the hydrogen atoms were calculated by using a C–H distance of 0.95 Å with β set at 8.0. Further full matrix least-squares refinement keeping the hydrogens in fixed positions while allowing the methylene chloride and the phenyl carbons to vary isotropically and the remaining atoms to vary anisotropically converged with R = 3.5% and R_w = 4.7%.[23] The largest peak in the final difference Fourier had an intensity of 0.74 e/Å^3 and was residual electron density around the tungsten.

Theoretical Calculations. The extended Hückel method, program ICON8, was used for calculations on the model complexes *fac*-$W(CO)_3(PH_3)_2(HCCH)$ and *mer*-$W(CO)_3(PH_3)_2(HCCH)$. Values for parameters used in the calculations were obtained from the literature.[24] Inner coordination sphere distances were taken from the structure of *mer*-$W(CO)_3$(dppe)(diethylfumarate).[25] The M–C(alkyne) and the C–C(alkyne) distances were set at 2.06 and 1.28 Å, respectively, as found in the structure of $W(CO)(PhCCPh)_3$.[8] The C–C–H angle was set at 135°.

Results

***fac*-$W(CO)_3$(dppe)$(\eta^2$-HC≡CR) [R = H (2a), Ph (2b), *n*-Bu (2c)].** These complexes were prepared by alkyne substitution of the labile solvent ligand in *fac*-$W(CO)_3$(dppe)(acetone).[17] Toluene was used as the reaction solvent, and the products were isolated after 5 min of stirring by filtering the reaction solution directly into excess hexanes to precipitate the alkyne adducts (eq 1). Tetrahydrofuran is also a suitable reaction solvent for preparing **2a** and **2b**, but addition of a large excess of 1-hexyne to *fac*-$W(CO)_3$(dppe)(acetone) in THF yields only a 1:1 equilibrium mixture of *fac*-$W(CO)_3$(dppe)(η^2-HC≡-*n*-Bu) and *fac*-$W(CO)_3$(dppe)(THF).

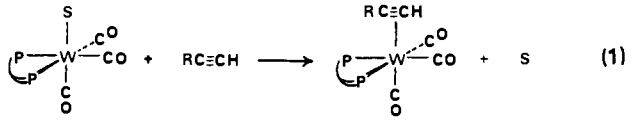

(1)

Replacement of coordinated acetone with phenylacetylene results in roughly a 50-cm^{-1} increase in the average carbonyl stretching frequency. A triplet at 5.74 ppm ($^3J_{HP}$ = 12 Hz) in the ^{1}H NMR is assigned to the terminal acetylenic proton which is coupled to both dppe phosphorus nuclei. Retention of a facial geometry is evident from the singlet, 37.6 ppm, observed in the ^{31}P spectrum of **2b**. This signal is accompanied by satellites due to ^{183}W ($I = {}^1/_2$, 14% abundant), $^1J_{PW}$ = 204 Hz, a value in the range observed for ^{31}P nuclei trans to carbonyl ligands in d^6 complexes.[26] Similar IR and ^{1}H NMR results were obtained for the acetylene and 1-hexyne adducts, **2a** and **2c**, respectively.

Addition of internal alkynes such as PhC≡CPh, MeC≡CMe, or EtC≡CEt to *fac*-$W(CO)_3$(dppe)(acetone) in toluene produced

(18) Zingales, F.; Canziani, F. *Gazzeta* **1962**, *92*, 343.

(19) Programs utilized during solution and refinement were from the Enraf-Nonius structure determination package.

(20) $I = S(C + RB)$ and $\sigma(I) = [2S^2(C + R^2B) + (\rho I)^2]^{1/2}$, where S = scan rate, C = total integrated peak count, R = ratio of scan count time to background count time, B = total background count, and ρ = 0.03 is a correction factor.

(21) The function minimized was $\Sigma w(|F_o| - |F_c|)^2$.

(22) $R_{unweighted} = \Sigma(|F_o| - |F_c|)/\Sigma|F_o|$ and $R_{weighted} = \Sigma|w(|F_o| - |F_c|)^2/\Sigma wF_o^2]^{1/2}$.

(23) Scattering factors were taken from the following: Cromer, D. T.; Waber, J. T. *International Tables for X-ray Crystallography*; Ibers, J. A., Hamilton, W. C., Eds.; Kynoch Press: Birmingham, England, 1974; Vol. IV, Table 2.2.

(24) (a) Hoffmann, R. *J. Chem. Phys.* **1963**, *39*, 1397. (b) Kubacek, P.; Hoffmann, R. *J. Am. Chem. Soc.* **1981**, *103*, 4320. (c) Stockis, A.; Hoffmann, R. *J. Am. Chem. Soc.* **1980**, *102*, 2952. (d) Schilling, B. E. R.; Hoffmann, R.; Lichtenberger, D. L. *J. Am. Chem. Soc.* **1979**, *101*, 585.

(25) Faller, J. W.; personal communication.

(26) Pregosin, P. S.; Kunz, R. W. *NMR: Basic Princ. Prog.* **1978**, *16*, 126. (b) Grim, S. O.; Wheatland, D. A.; McFarlane, W. *J. Am. Chem. Soc.* **1967**, *89*, 5573. (c) Birdwhistell, K. R.; Tonker, T. L.; Templeton, J. L. *J. Am. Chem. Soc.* **1985**, *107*, 4474.

Table II. Atomic Positional Parameters for $W(CO)_2(dppe)(DMAC)_2$ (**3**)[a]

atom	x	y	z
W	0.22019 (2)	0.23095 (1)	0.9729 (2)
P(1)	0.3021 (1)	0.18376 (7)	0.3287 (1)
P(2)	0.2432 (1)	0.35171 (7)	0.2662 (1)
O(1)	0.0753 (4)	0.3031 (2)	−0.1670 (4)
O(2)	0.2531 (4)	0.0813 (3)	−0.1079 (4)
O(3)	0.3376 (4)	0.3080 (3)	−0.1765 (4)
O(4)	0.5243 (4)	0.2769 (3)	−0.0453 (4)
O(5)	0.5941 (4)	0.2464 (2)	0.3170 (4)
O(6)	0.5987 (3)	0.1470 (2)	0.1545 (4)
O(7)	0.0094 (5)	0.0707 (3)	−0.0729 (7)
O(8)	−0.1402 (4)	0.1450 (3)	−0.0103 (5)
O(9)	−0.0139 (4)	0.3022 (2)	0.3504 (4)
O(10)	−0.1480 (3)	0.3100 (2)	0.1431 (4)
C(1)	0.1264 (5)	0.2774 (3)	−0.0712 (5)
C(2)	0.2413 (5)	0.1342 (3)	−0.0313 (5)
C(3)	0.3619 (5)	0.2569 (3)	0.0239 (5)
C(4)	0.4176 (5)	0.2256 (3)	0.1312 (5)
C(5)	0.4032 (5)	0.2841 (3)	−0.0769 (5)
C(6)	0.5792 (6)	0.3001 (5)	−0.1378 (7)
C(7)	0.5449 (5)	0.2091 (3)	0.2110 (5)
C(8)	0.7236 (6)	0.1247 (4)	0.2329 (8)
C(9)	0.0513 (5)	0.0862 (3)	0.0605 (5)
C(10)	0.0455 (4)	0.2470 (3)	0.1468 (5)
C(11)	−0.0254 (5)	0.1273 (3)	−0.0146 (6)
C(12)	−0.2239 (7)	0.0922 (4)	−0.0893 (9)
C(13)	−0.0393 (5)	0.2884 (3)	0.2255 (5)
C(14)	−0.2343 (6)	0.3561 (4)	0.2146 (8)
C(15)	0.3648 (5)	0.2612 (3)	0.4614 (5)
C(16)	0.2812 (5)	0.3325 (3)	0.4432 (5)
C(17)	0.1938 (5)	0.1515 (3)	0.3954 (5)
C(18)	0.1707 (5)	0.1816 (3)	0.5233 (5)
C(19)	0.0907 (6)	0.1527 (3)	0.5665 (6)
C(20)	0.0326 (6)	0.0941 (3)	0.4867 (6)
C(21)	0.0524 (6)	0.0639 (3)	0.3570 (6)
C(22)	0.1324 (5)	0.0932 (3)	0.3132 (5)
C(23)	0.4292 (5)	0.1095 (3)	0.3482 (5)
C(24)	0.5266 (6)	0.1088 (3)	0.4696 (6)
C(25)	0.6256 (7)	0.0495 (4)	0.4794 (7)
C(26)	0.6119 (7)	−0.0075 (4)	0.3723 (7)
C(27)	0.5170 (6)	−0.0082 (4)	0.2522 (6)
C(28)	0.4267 (5)	0.050 (3)	0.2407 (5)
C(29)	0.1141 (5)	0.4244 (3)	0.2594 (5)
C(30)	0.0191 (6)	0.4275 (3)	0.1403 (6)
C(31)	−0.0770 (7)	0.4846 (4)	0.1340 (8)
C(32)	−0.0772 (7)	0.5385 (4)	0.2454 (7)
C(33)	0.0176 (7)	0.5378 (4)	0.3655 (7)
C(34)	0.1124 (6)	0.4806 (4)	0.3734 (6)
C(35)	0.3619 (5)	0.4034 (3)	0.2630 (5)
C(36)	0.4713 (5)	0.4120 (3)	0.3662 (6)
C(37)	0.5543 (6)	0.4549 (4)	0.3546 (7)
C(38)	0.5301 (7)	0.4867 (4)	0.2425 (7)
C(39)	0.4237 (7)	0.4759 (4)	0.1346 (7)
C(40)	0.3408 (6)	0.4345 (3)	0.1441 (6)
C(41)	0.1957 (7)	0.7096 (4)	0.4008 (8)
Cl(1)	0.1887 (2)	0.7836 (1)	0.3208 (3)
Cl(2)	0.2607 (3)	0.6288 (1)	0.3167 (3)

[a] Numbers in parentheses are the esd's of the last digit listed.

mixtures of carbonyl containing products as judged by solution infrared spectra. Weak carbonyl IR absorptions compatible with *fac*-$W(CO)_3(dppe)(\eta^2\text{-}RC{\equiv}CR)$ formulations were present in solution, but we were unable to purify and isolate these products. No reaction was evident when the labile molybdenum complex, *fac*-$Mo(CO)_3(dppe)(THF)$ was added to a large excess of phenylacetylene.

$W(CO)_2(dppe)(DMAC)_2$ (3) [DMAC = Dimethylacetylenedicarboxylate]. Addition of DMAC to a THF solution of *fac*-$W(CO)_3(dppe)$(acetone) forms $W(CO)_2(dppe)(DMAC)_2$ (eq 2).

$$\textit{fac}\text{-}W(CO)_3(dppe)(\text{acetone}) + 2DMAC \rightarrow W(CO)_2(dppe)(DMAC)_2 + CO(g) + Me_2CO \quad (2)$$

The facial tricarbonyl infrared absorptions of the reagent are replaced by cis dicarbonyl absorptions approximately 100 cm^{-1} above those of the starting material. The IR also shows two

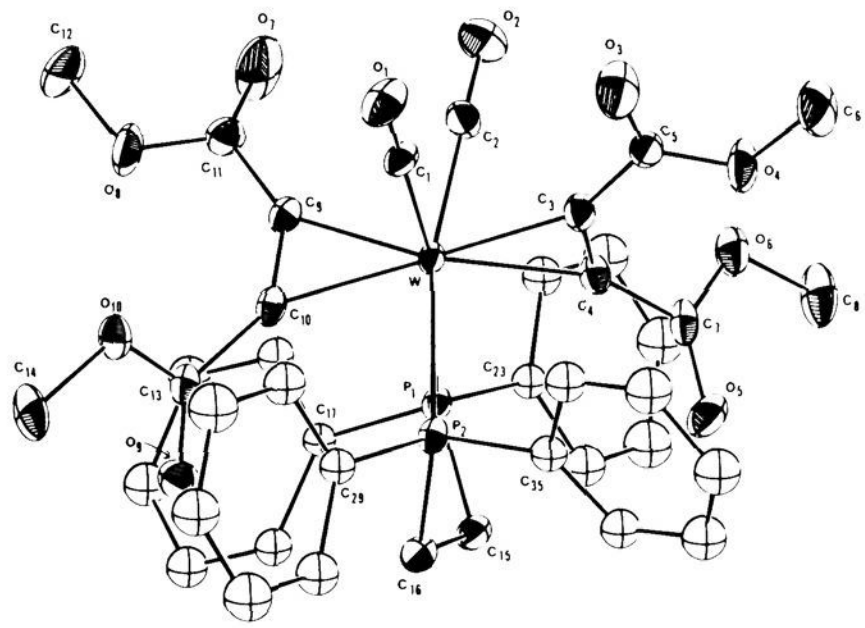

Figure 1. An ORTEP of $W(CO)_2(dppe)(DMAC)_2$ (**3**) illustrating the atomic numbering scheme.

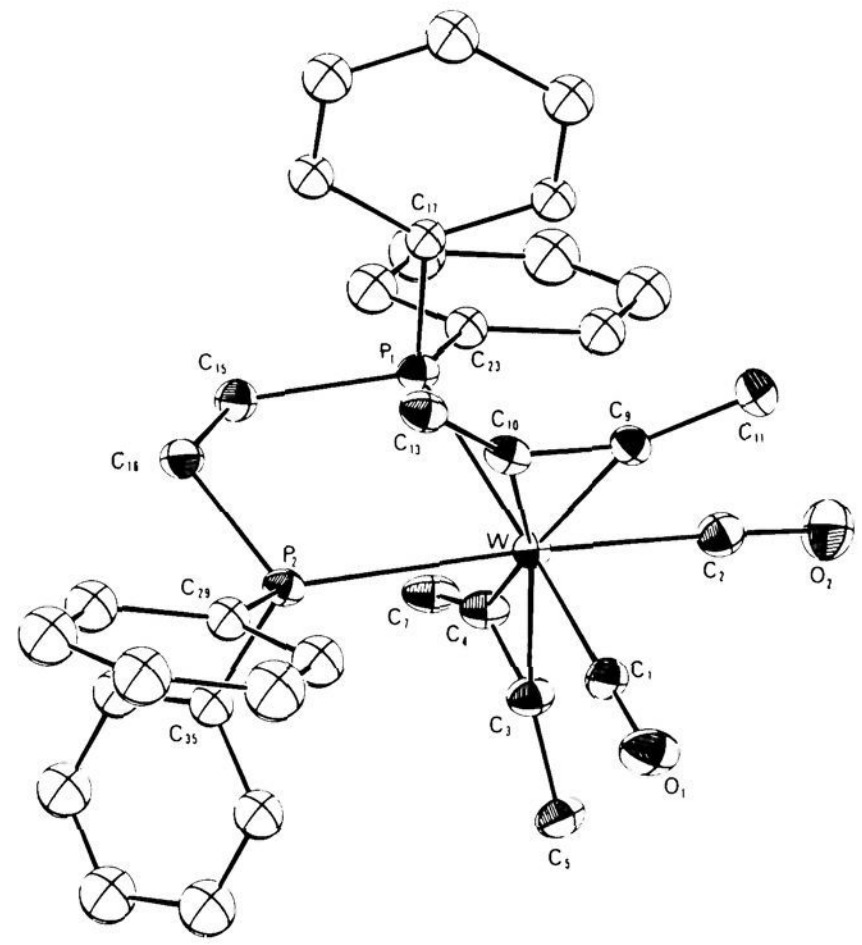

Figure 2. A view of the staggered-eclipsed inner coordination sphere of $W(CO)_2(dppe)(DMAC)_2$ (**3**). The four DMAC ester O_2Me groups have been removed for clarity.

medium intensity absorptions at 1730 and 1700 cm^{-1} due to alkyne ester substituents. Singlets at 3.58 and 2.74 ppm in the ^1H NMR spectrum of **3** are assigned to the methoxy groups of the alkyne ligands. Both dppe ^{31}P nuclei resonate at 27.5 ppm with $^1J_{PW}$ = 187 Hz in the ^{31}P NMR spectrum of **3**. The cis dicarbonyl infrared pattern and equivalent environments for both ends of the chelating dppe ligand are only consistent with a trans arrangement of the two alkyne ligands. The two equivalent carbonyl carbons appear at 202.0 ppm in the ^{13}C spectrum as a doublet ($^2J_{CP}$ = 61 Hz) due to strong coupling to the trans phosphorus nucleus. ^{13}C singlets were assigned to the ester carbonyls (170.6 and 166.5 ppm) and the alkyne methoxy carbons (52.3 and 51.2 ppm), but we were unable to identify the alkyne carbons; they may be obscured by the dppe phenyl resonances.

The trans alkyne–cis carbonyl geometry for **3** anticipated from spectral data was confirmed by the solid-state structure shown in Figure 1 where the atomic numbering scheme is defined. The inner coordination sphere is seen more clearly in Figure 2. Final positional parameters for all non-hydrogen atoms are listed in Table II, while bond distances and angles are collected in Tables III and IV, respectively.

Table III. Selected Bond Distances (Å) in $W(CO)_2(dppe)(DMAC)_2$ (**3**)

W–P(1)	2.565 (1)
W–P(2)	2.542 (1)
W–C(1)	2.033 (3)
W–C(2)	2.033 (3)
W–C(3)	2.162 (3)
W–C(4)	2.177 (3)
W–C(9)	2.150 (3)
W–C(10)	2.176 (3)
P(1)–C(15)	1.846 (3)
P(1)–C(17)	1.835 (3)
P(1)–C(23)	1.838 (3)
P(2)–C(16)	1.837 (3)
P(2)–C(29)	1.834 (3)
P(2)–C(35)	1.824 (3)
C(1)–O(1)	1.143 (4)
C(2)–O(2)	1.144 (4)
C(5)–O(3)	1.197 (4)
C(5)–O(4)	1.320 (4)
C(6)–O(4)	1.463 (4)
C(7)–O(5)	1.193 (4)
C(7)–O(6)	1.330 (4)
C(8)–O(6)	1.455 (5)
C(11)–O(7)	1.175 (5)
C(11)–O(8)	1.317 (4)
C(12)–O(8)	1.444 (5)
C(13)–O(9)	1.203 (4)
C(13)–O(10)	1.331 (4)
C(14)–O(10)	1.466 (4)
C(3)–C(4)	1.303 (4)
C(3)–C(5)	1.477 (4)
C(4)–C(7)	1.459 (5)
C(9)–C(10)	1.292 (4)
C(9)–C(11)	1.468 (5)
C(10)–C(13)	1.469 (4)
C(15)–C(16)	1.524 (5)

Cyclic Voltammetry. Oxidation potentials for the three *fac*-$W(CO)_3(dppe)(HCCR)$ complexes and $W(CO)_2(dppe)(DMAC)_2$ are compiled in Table V. In the *fac*-$W(CO)_3(dppe)(HCCR)$ series a reversible oxidation is observed near +0.2 V. A second oxidation, usually irreversible, is alkyne dependent. No reductions were observed. In contrast to **2a–c**, $W(CO)_2(dppe)(DMAC)_2$ has its first oxidation near +0.8 V, consistent with a much lower energy HOMO in this complex relative to the three *fac*-$W(CO)_2$-(dppe)(HCCR) complexes.

Discussion

Reactivity Patterns. Octahedral d^6 metal complexes have no vacant $d\pi$ orbitals, and we anticipated that a repulsive 4-electron-2-center $d\pi-\pi_\perp$ conflict would characterize d^6 $L_5M(\eta^2$-alkyne) complexes. Terminal alkynes can undergo isomerization to form vinylidene complexes (eq 3)[27] to eliminate $d\pi$–ligand π conflicts.[28] This alkyne to vinylidene rearrangement, common for octahedral d^6 complexes, has not been observed for octahedral d^4 alkyne complexes where there is no 4-electron $d\pi-\pi_\perp$ conflict.

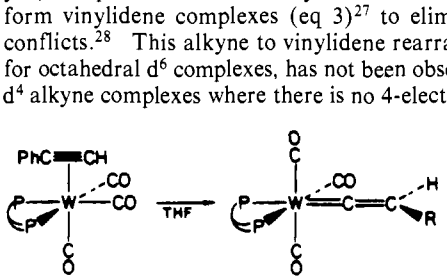

(3)

Preliminary efforts with $[Et_4N][Mo(CO)_5Cl]$ as a precursor to d^6 alkyne derivatives appeared to yield $[Et_4N][Mo(DMAC)_3Cl]$, a four-coordinate complex analogous to $M(RC{\equiv}CR)_3L$ complexes reported by others.[7,29] The electron withdrawing ester groups of DMAC evidently promote additional CO loss once DMAC enters the coordination sphere (vide infra). Alkynes such as PhC_2Ph and PhC_2H did not react with $[Mo(CO)_5Cl]^-$.

Table IV. Selected Bond Angles (deg) in $W(CO)_2(dppe)(DMAC)_2$ (**3**)

P(1)–W–P(2)	80.2 (1)
P(1)–W–C(1)	168.7 (1)
P(1)–W–C(2)	97.9 (1)
P(1)–W–C(3)	113.9 (1)
P(1)–W–C(4)	79.3 (1)
P(1)–W–C(9)	89.2 (1)
P(1)–W–C(10)	83.2 (1)
P(2)–W–C(1)	94.7 (1)
P(2)–W–C(2)	167.7 (1)
P(2)–W–C(3)	86.9 (1)
P(2)–W–C(4)	84.9 (1)
P(2)–W–C(9)	115.3 (1)
P(2)–W–C(10)	80.6 (1)
C(1)–W–C(2)	89.2 (1)
C(1)–W–C(3)	75.6 (1)
C(1)–W–C(4)	110.5 (1)
C(1)–W–C(9)	83.9 (1)
C(1)–W–C(10)	86.0 (1)
C(2)–W–C(3)	82.7 (1)
C(2)–W–C(4)	82.8 (1)
C(2)–W–C(9)	76.7 (1)
C(2)–W–C(10)	111.5 (1)
C(3)–W–C(4)	34.9 (1)
C(3)–W–C(9)	151.0 (1)
C(3)–W–C(10)	156.8 (1)
C(4)–W–C(9)	154.8 (1)
C(4)–W–C(10)	158.9 (1)
C(9)–W–C(10)	34.8 (1)
C(4)–C(3)–C(5)	134.5 (3)
C(3)–C(4)–C(7)	135.9 (3)
C(10)–C(9)–C(11)	138.9 (3)
C(9)–C(10)–C(13)	137.5 (3)
C(5)–O(4)–C(6)	117.4 (3)
C(7)–O(6)–C(8)	115.6 (3)
C(11)–O(8)–C(12)	115.9 (3)
C(13)–O(10)–C(14)	115.3 (3)
O(3)–C(5)–O(4)	123.3 (3)
O(3)–C(5)–C(3)	125.7 (3)
O(4)–C(5)–C(3)	111.0 (3)
O(5)–C(7)–O(6)	123.8 (3)
O(5)–C(7)–C(4)	123.7 (3)
O(6)–C(7)–C(4)	112.4 (3)
O(7)–C(11)–O(8)	122.8 (3)
O(7)–C(11)–C(9)	125.0 (3)
O(8)–C(11)–C(9)	112.2 (3)
O(9)–C(13)–O(10)	123.3 (3)
O(9)–C(13)–C(10)	124.3 (3)
O(10)–C(13)–C(10)	112.4 (2)

Table V. Cyclic Voltammetry Data

complex	$E_{p/2}$ (ox) V[a]	ΔE, (mV)[b]	i_c/i_a
fac-$W(OC)_3(dppe)(HCCH)$ (**2a**)	+0.22, +0.67	85	0.9
fac-$W(OC)_3(dppe)(HCCPh)$[c] (**2b**)	+0.2, +0.35[c]	120, 110	*c*
fac-$W(OC)_3(dppe)(HCCBu)$ (**2c**)	+0.18, +0.63	90	1.0
trans-$W(DMAC)_2(dppe)(CO)_2$ (**3**)	+0.78		

[a] Potentials are reported relative to a saturated sodium chloride calomel electrode (SSCE) by using a value of +0.42 V for the ferrocene couple. Irreversible waves are reported as the potential at half peak height. [b] This is the peak-to-peak separation for the reversible oxidative waves (i.e., i_c/i_a, the ratio of cathodic current to anodic current, was between 0.9 and 1.0). [c] This voltammogram was recorded at −78 °C. The two oxidative waves were not separated well enough to obtain an accurate i_c/i_a ratio.

(27) (a) Bruce, M. I.; Swincer, A. G. *Adv. Organomet. Chem.* **1983**, *22*, 59. (b) Adams, J. S.; Cunningham, M.; Whiteley, M. W. *J. Organomet. Chem.* **1985**, *293*, C13. (c) Pombeiro, A. J. L.; Jeffery, J. C.; Pickett, C. J.; Richards, R. L. *J. Organomet. Chem.* **1984**, *277*, C7.

(28) Birdwhistell, K. R.; Burgmayer, S. J. N.; Templeton, J. L. *J. Am. Chem. Soc.* **1983**, *105*, 7789.

(29) (a) Maher, J. M.; Fox, J. R.; Foxman, B. M.; Cooper, N. J. *J. Am. Chem. Soc.* **1984**, *106*, 2347. (b) Chiu, K. W.; Lyons, D.; Wilkinson, G.; Thornton-Pett, M.; Hursthouse, M. B. *Polyhedron* **1983**, *2*, 803.

In order to avoid pseudotetrahedral trisalkyne d^6 products we introduced a bis(diphenylphosphino)ethane chelate into the coordination sphere of the d^6 metal reagent. Using *fac*-$W(CO)_3$(dppe)(acetone) as a precursor to *fac*-$W(CO)_3$(dppe)L derivatives we prepared several olefin complexes (L = maleic anhydride, diethyl maleate, diethyl fumarate) prior to attempting isolation of alkyne derivatives. During the course of our studies, Schenk and co-workers reported an extensive Group 6 olefin chemistry, including kinetics for the *fac* to *mer* rearrangements observed with electron deficient olefins in $M(CO)_3$(dppe)(η^2-olefin) complexes.[17]

Addition of alkyne to *fac*-$W(CO)_3$(dppe)(acetone) in THF or toluene produced the desired alkyne adducts. These alkyne complexes are labile, and the solutions were cooled rapidly to 0 °C after formation to avoid decomposition or isomerization to vinylidene products. The alkyne ligands in the *fac*-$W(CO)_3$(dppe)(η^2-HC≡CR) series are easily displaced relative to alkynes in d^4 octahedral complexes. For comparison *fac*-$W(CO)_3$(dppe)(η^2-HC≡CPh) immediately forms a 1:1 mixture of reagent and *fac*-$W(CO)_3$(dppe)(THF) upon dissolution in THF at room temperature, while $(PEt_3)_2(OC)Br_2Mo(\eta^2$-HC≡CPh) resists alkyne substitution by phosphine reagents in refluxing toluene.

Other octahedral d^6 complexes also have labile alkynes: (π-C_5H_5)$(OC)_2Mn(\eta^2$-RC≡CR) complexes readily dissociate the alkyne ligand,[13] and Reger has noted that alkyne ligands in [(π-C_5H_5)$(OC)_2Fe(\eta^2$-RC≡CR)]$^+$ can be displaced by acetone.[14a] Geoffroy recently reported reactive d^6 carbene–alkyne complexes. Low-temperature photolysis of $(OC)_5W$=C(OMe)Ph in the presence of alkynes produces spectroscopically observable alkyne adducts, but only the diphenylacetylene derivative was isolated as a solid.[30] Another example of a stable six-coordinate d^6 alkyne derivative, (π-C_5H_5)$(OC)_2Re(\eta^2$-PhC≡CPh), was recently reported.[15] It seems that diphenylacetylene is a viable ligand in d^6 complexes where alkyl or terminal alkyne analogues resist isolation. Numerous DMAC complexes also exist,[31] and $W(CO)_2$(dppe)$(DMAC)_2$ provides another example where analogous alkyl or aryl alkynes do not yield a similar product. Clearly electron-withdrawing alkyne substituents favor retention of the alkyne in d^6 metal coordination spheres.

Of the three terminal alkyne adducts isolated, only the phenylacetylene adduct, **2b**, isomerized cleanly to the vinylidene derivative, *mer*-$W(CO)_3$(dppe)=C=C(H)Ph.[28] Cationic [(π-C_5H_5)$L_2Ru(\eta^2$-HC≡CR)]$^+$ complexes readily isomerize to vinylidene ligands for alkyl, aryl, and ester R groups.[27,32] Decomposition of **2a** or **2c** in THF at room temperature produced (dppe)$W(CO)_4$ as the only soluble carbonyl species and precipitated $W(CO)_3$(dppe)$P(Ph)_2CH_2CH_2(Ph)_2$P-$W(CO)_3$(dppe) as a pale yellow powder. These two products were also observed when internal alkynes were added to *fac*-$W(CO)_3$(dppe)(acetone) in thf. The kinetic stability of the alkyne adducts decreases as the steric bulk of the alkyne substituents increases, i.e., HC_2H is more stable than HC_2Ph, followed by $HC_2(CH_2)_3CH_3$.

Only the $W(CO)_2$(dppe)$(DMAC)_2$ complex withstood chromatographic purification; **2a–c** decomposed on Florisil. The importance of electron-withdrawing substituents on alkyne ligands has been recognized for some time, and lowering the energy of the alkyne $\pi_\parallel$* orbitals to enhance metal dπ backbonding has been discussed. For these d^6 octahedral complexes the carboxylate groups can provide additional stability by delocalizing the alkyne $\pi_\perp$ electron pair away from the filled metal dπ orbital it confronts to decrease the antibonding dπ–$\pi_\perp$ conflict.

Structure of $W(CO)_2$(dppe)$(DMAC)_2$. The geometry of **3** is nearly octahedral. The most interesting geometric features are the orientations of the two trans alkyne ligands relative to one another and relative to the P–W–CO vectors. The two alkynes are mutually orthogonal (92.1°), and each alkyne nearly eclipses one of the P–W–CO vectors (8.8 and 1.8°). The staggered geometry allows these two strong single-faced π-acid ligands to overlap different filled dπ orbitals. Orthogonal orientations for trans single faced π-acids or π-donors are common[33] and have been discussed theoretically.[34]

The energy considerations which favor positioning alkyne C≡C axes over equatorial metal–ligand bonds are more subtle. Both steric and electronic factors were invoked in a theoretical study of *trans*-$(H_2C{=}CH_2)_2Mo(PH_3)_4$, but steric factors for the alkynes in **3** should favor locating the alkynes 45° off axis between the equatorial ligand positions. Repulsion of the filled d_{xy} metal orbital with the filled C_2 $\pi_\parallel$ donor orbital has been cited as an electronic term favoring the eclipsed geometry where $\pi_\parallel$ encounters the filled $d_{x^2-y^2}$ σ bonding orbital which is less repulsive due to both overlap and energy factors than is d_{xy}.[35] The same feature may be operative here.

Average values for the geometries of the alkynes in **3** will be employed for comparison with $[Ru(NH_3)_5(DMAC)][PF_6]_2$.[36] The longer C≡C distance (1.30 Å cf. 1.24 Å), the lower ν(C≡C) frequency (1895 cm^{-1} cf. 1947 cm^{-1}), and the bend back angles (137 ± 2° cf. 148 ± 4°) for W(0) relative to Ru(II) reflect stronger metal alkyne bonding in the tungsten derivative. The M–C distances are not directly comparable, but if you estimate that Ru(II) is 0.17 Å smaller than W(0) based on average metal carbonyl M–C bond lengths,[37] the average 2.17 Å value for W–C also implies tighter binding than the 2.13 Å average Ru–C distance.

The reason for belaboring this W/Ru comparison stems from the propensity for backbonding from the d^6 $Ru(NH_3)_5^{2+}$ fragment, a premiere metal dπ donor. Expectations for two-electron alkyne bonding based on $\pi_\parallel$ donation and $\pi_\parallel$* acceptance are inadequate here. Donation from Ru(II) dπ to $\pi_\parallel$* should weaken the C≡C bond, but in fact the tungsten center clearly perturbs the free alkyne more substantially. We suggest that the dπ orbital extension and energy of $Ru(NH_3)_5^{2+}$ which promote coordination of N_2[38] actually inhibit tight binding of alkynes due to increased ligand $\pi_\perp$-metal dπ repulsion.

The individual contributions of two π effects—increased alkyne $\pi_\parallel$* acidity vs. decreased alkyne $\pi_\perp$ basicity—are difficult to probe spectroscopically. Luckily the orientation of the carboxylate groups directly addresses this question. The angle between the M–C_2 metal–alkyne plane and the CO_2 carboxylate plane determines the distribution of ester delocalization between $\pi_\parallel$* and $\pi_\perp$. The ester groups on C3 and C9 lie near the metal alkyne planes (4° and 14°, respectively) and overlap with $\pi_\perp$ orbitals. The esters attached to C4 and C10, alkyne carbons above the PPh_2 groups (see Figure 2) and more likely to encounter steric restrictions, form angles of 99° and 120° with their respective metal–alkyne planes. Thus the ester groups with greater rotational freedom choose to align with the $\pi_\perp$ alkyne orbitals and decrease $\pi_\perp$–dπ repulsion rather than to align with $\pi_\parallel$* orbitals to enhance backbonding to $\pi_\parallel$*. In (π-C_5H_5)$(OC)_2Re(PhC{\equiv}CPh)$ the rings are canted less than 20° from the ReC_2 plane, again favoring overlap with $\pi_\perp$ rather than $\pi_\parallel$*.[15]

Infrared Properties. The π-acidity of alkyne ligands is reflected in ν_{CO} frequencies. The average ν_{CO} frequency of *fac*-$W(CO)_3$(dppe)(L) increases by more than 30 cm^{-1} when THF is replaced by HC_2R. The order of π-acidity for HC_2R is R = Bu < H < Ph. Although the stoichiometry difference between **2** and **3** makes

(30) Foley, H. C.; Strubinger, L. M.; Targos, T. S.; Geoffroy, G. L. *J. Am. Chem. Soc.* **1983**, *105*, 3064.
(31) (a) Bowden, F. L.; Lever, A. B. P. *Organomet. Chem. Rev.* **1968**, *3*, 227. (b) Sullivan, B. P.; Smythe, R. S.; Kober, E. M.; Meyer, T. J. *J. Am. Chem. Soc.* **1982**, *104*, 4701.
(32) Bruce, M. I.; Wallis, R. C. *Aust. J. Chem.* **1979**, *32*, 1471.
(33) (a) Carmona, E.; Marin, J. M.; Poveda, M. L.; Atwood, J. L.; Rogers, R. D. *J. Am. Chem. Soc.* **1983**, *105*, 3014. (b) Angermund, K.; Grevels, F.-W.; Kruger, E. C.; Skibbe, V. *Angew. Chem., Int. Ed. Engl.* **1984**, *23*, 904. (c) Byrne, J. W.; Blaser, H. U.; Osborn, J. A. *J. Am. Chem. Soc.* **1975**, *97*, 3871. (d) Alvarez, R.; Carmona, E.; Marin, J. M.; Poveda, M. L.; Gutierrez-Puebla, E.; Monge, A. *J. Am. Chem. Soc.* **1986**, *108*, 2286.
(34) (a) Bachmann, C.; Demuynck, J.; Veillard, A. *J. Am. Chem. Soc.* **1978**, *100*, 2366. (b) Rösch, N.; Hoffmann, R. *Inorg. Chem.* **1974**, *13*, 2656.
(35) Albright, T. A.; Hoffmann, R.; Thibeault, J. C.; Thorn, D. L. *J. Am. Chem. Soc.* **1979**, *101*, 3801.
(36) Henderson, W. W.; Bancroft, B. T.; Shepherd, R. E.; Fackler, J. P., Jr. *Organometallics* **1986**, *5*, 506.
(37) (a) Lukehart, C. M. *Fundamental Transition Metal Organometallic Chemistry*; Brooks/Cole: Belmont, CA, 1985. (b) Seddon, K. R.; Seddon, E. A. *The Chemistry of Ruthenium*; Elsevier: 1984.
(38) Allen, A. D.; Bottomley, F. *Acc. Chem. Res.* **1968**, *1*, 360.

direct comparison of HC_2R and DMAC alkynes impossible, the average CO frequency of 2005 cm^{-1} for **3** with only two carbonyl ligands is roughly 100 cm^{-1} above the average of the facial alkyne complexes with three carbonyl ligands. This data reinforces the role of DMAC as a ligand comparable to CO in π-acid strength.[36,39] That ester substituents promote $d\pi$ to $\pi_{\parallel}^*$ back-bonding and reduce $\pi_{\perp}$–$d\pi$ conflicts is also evident in the much more positive oxidation potential of **3** relative to **2a–c**. Note that Cooper and co-workers have reported two-electron reduction of $Cr(C_4Ph_4)(PhC_2Ph)(CO)_2$ to a dianion with retention of all ligands.[10b]

The $W(CO)_2(dppe)(DMAC)_2$ complex has a weak IR absorption at 1895 cm^{-1} which we assign to the acetylenic C≡C stretch. This frequency falls in the $\nu_{C\equiv C}$ range common for d^6 octahedral alkyne complexes[31,39] and is higher than values reported for Mo(IV) (1850–1870 cm^{-1})[3a] and Mo(II) (1790–1820)[2c] DMAC complexes. This data is compatible with retention of more carbon–carbon triple bond character in d^6 complexes than in cases where a vacant metal $d\pi$ orbital invites constructive donation from the C≡C $\pi_{\perp}$ bonding orbital. We were unable to locate (C≡C) stretches in **2a–c**; they may well lie under intense carbonyl bands in the 1850–1950-cm^{-1} region.

***fac*-(dppe)$(OC)_3W(\eta^2$-HC≡CR) NMR Properties.** Chemical shift values for acetylenic protons and carbons have been empirically correlated with alkyne $\pi_{\perp}$ donation to molybdenum and tungsten. Terminal alkyne proton chemical shift values have been broadly categorized as four-electron donor alkynes (≈12–13 ppm), three-electron donor alkynes (≈10–11 ppm), and two-electron donor alkynes (≈7–8 ppm).[4b] The acetylenic hydrogens of **2a**, **2b**, and **2c** appear at 5.78, 5.74, and 4.49 ppm, respectively. These shifts are well above formal two-electron donor alkynes in d^4 $(\pi$-$C_5H_5)_2Mo(\eta^2$-HC≡CR) complexes[40] and are approaching free alkyne values (2–3 ppm) relative to more tightly bound alkyne ^1H chemical shifts.

Bound alkynes ^{13}C chemical shifts vary over nearly 200 ppm;[41] rough guidelines are four-electron donors (≈190–250 ppm), three-electron donors (≈130–170 ppm), and two-electron donors (≈100–120 ppm). The extreme lability of adducts **2a–c** limited our ability to obtain ^{13}C spectra, but the phenylacetylene complex **2b** exhibited resonances at 98.2 and 88.7 ppm assigned as the bound alkyne carbons (cf. free HC≡CPh, 82.4 and 76.5 ppm). Even higher ^{13}C chemical shifts have been reported for other d^6 alkyne complexes.[15]

Alkyne coupling constants here also reflect weak metal–alkyne bonding. The $^1J_{CH}$ value of 231 Hz for **2b** lies nearly midway between free phenylacetylene (251 Hz) and complexed phenylacetylene in $W(CO)(S_2CNR_2)(RC_2H)$ (210 Hz)[42] and $W(O)(S_2CNR_2)_2(RC_2H)$ (215 Hz).[4b] For comparison the bridging HC≡CH ligand in $W_2(O$-t-$Bu)_6(py)(\mu$-$C_2H_2)$ has a long C–C bond length of 1.44 Å and a $^1J_{CH}$ of 192 Hz.[43] The $^2J_{CH}$ coupling constant of 27 Hz in **2b** is also large relative to $^2J_{CH}$ values of 11 and 7 Hz seen in $W(CO)(S_2CNR_2)_2(HC\equiv CH)$ and $W(O)(S_2CNR_2)_2(HC\equiv CH)$.

The ^1H NMR spectrum of *fac*-$W(CO)_3(dppe)(\eta^2$-HC≡CH) exhibits a triplet at 5.78 ppm ($^3J_{HP}$ = 4 Hz) which integrates for two protons and remains unchanged down to −95 °C. Although a static structure with equivalent alkyne ends is possible as in III below, we favor rapid alkyne rotation to account for the single signal observed (I or II). Extended Huckel molecular orbital calculations which favor alignment of the C≡C linkage parallel to a OC–W–P vector produce a low calculated rotational barrier of 8.4 kcal/mol. The $^3J_{HP}$ of 4 Hz observed for **2a** is small relative to the 11 and 12 Hz values in the unsymmetrical terminal alkyne complexes, **2b** and **2c**. The HC≡CPh and HC≡C-*n*-Bu complexes may well position the large alkyne substituent in the sterically less demanding site such that the only isomer which is substantially populated has a large $^3J_{HP}$. The parent acetylene derivative then places a proton in each environment, and the observed 4 Hz triplet coupling represents the average of one large and one small, probably of opposite sign, $^3J_{HP}$ coupling constant.

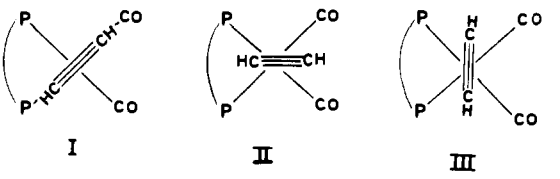

$W(CO)_2$(dppe)$(DMAC)_2$ NMR Properties. Two singlets were observed for the four DMAC methoxy groups of **3** at room temperature. Heating caused coalescence, and only one methoxy signal was observed at 119 °C. These results are consistent with a static geometry at ambient temperatures which has two equivalent alkynes, with each alkyne having inequivalent ends (see Figure 2). Alkyne rotation with increasing temperature ultimately yields only one signal. The experimental barrier to alkyne rotation was calculated to be 17.7 kcal/mol for **3**,[44] quite close to the olefin rotational barrier in *trans*-$W(CO)_4(\eta^2$-olefin$)_2$.[45]

Summary. When will alkynes serve as simple two-electron donor olefin analogues? Electron-withdrawing substituents promote two-electron donation by delocalizing $\pi_{\perp}$ electrons away from filled metal $d\pi$ orbitals. Single faced substituents, e.g., esters, are particularly well suited for these interactions, and numerous DMAC complexes fall under the 18-electron umbrella as olefin analogues. Other common two-electron donor alkyne ligands include PhC≡CPh and $CF_3C\equiv CCF_3$.

When will terminal alkyne ligands rearrange to vinylidenes? Octahedral d^6 complexes containing a terminal alkyne ligand can eliminate the unfavorable $\pi_{\perp}$–$d\pi$ four-electron conflict by isomerization to form a vinylidene ligand, and they do. Octahedral d^4 or d^2 metal derivatives favor HC_2R as ligands relative to the M=C=CHR isomers.

When are terminal or dialkyl alkynes viable ligands? The relatively electron rich dialkylalkynes are good ligands and promote constructive $\pi_{\perp}$ donation in d^4 and d^2 octahedral derivatives. Isolation of dialkylalkyne complexes proved elusive in our efforts with d^6 tungsten reagents, probably reflecting both electronic and steric problems. Likewise HC≡CH is a better ligand in high oxidation state metal complexes with vacant metal $d\pi$ orbitals.

Acknowledgment. This work was supported by NSF Grant CHE8521840 and PRF Grant 13547-AC3. We are grateful to Professor D. J. Hodgson for crystallographic assistance.

Supplementary Material Available: Tables of thermal parameters, complete bond distances and angles, and calculated hydrogen positions for **3** (8 pages); listings of observed and calculated structure factors for **3** (24 pages). Ordering information is given on any current masthead page.

(39) Sullivan, B. P.; Kober, E. M.; Meyer, T. J. *Organometallics* **1982**, *1*, 1011.
(40) Thomas, J. L. *Inorg. Chem.* **1978**, *17*, 1507.
(41) Templeton, J. L.; Ward, B. C. *J. Am. Chem. Soc.* **1980**, *102*, 3288.
(42) Ward, B. C.; Templeton, J. L. *J. Am. Chem. Soc.* **1980**, *102*, 1532.
(43) Chisholm, M. H.; Folting, K.; Hoffman, D. M.; Huffman, J. C. *J. Am. Chem. Soc.* **1984**, *106*, 6794.
(44) (a) Faller, J. W. *Adv. Organomet. Chem.* **1977**, *16*, 211. (b) Templeton, J. L. *Adv. Chem. Ser.* **1979**, *173*, 263.
(45) Grevels, F.-W.; Lindeman, M.; Benn, R.; Goddard, R.; Krüger, C. *Z. Naturforsch, B: Anorg. Chem., Org. Chem.* **1980**, *B35*, 1298.